

Thermal Suppression of Strong Pinning

Orlando S. Wagner, Guido Burkard, Vadim B. Geshkenbein, and Gianni Blatter
Theoretische Physik, ETH-Hönggerberg, CH-8093 Zürich, Switzerland
 (6 March 1998)

We study vortex pinning in layered type-II superconductors in the presence of uncorrelated disorder for decoupled layers. Introducing the new concept of variable-range thermal smoothing, we describe the interplay between strong pinning and thermal fluctuations. We discuss the appearance and analyze the evolution in temperature of two distinct non-linear features in the current-voltage characteristics. We show how the combination of layering and electromagnetic interactions leads to a sharp jump in the critical current for the onset of glassy response as a function of temperature.

PACS numbers: 74.60.Ge, 74.60.Jg

Quenched disorder in strongly layered superconductors, such as the Bi-based high- T_c compounds or the organic BEDT-based materials, naturally leads to the phenomenon of strong vortex pinning. With the magnetic field directed perpendicular to the layers the vortex lines divide up into loosely coupled strings of “pancake” vortices [1]. At low fields, the absence of interactions between the pancake vortices allows for their free accommodation to the pinning potential, thus leading to strong pinning of individual pancake vortices. This is in contrast to the weak collective pinning situation [2], where the disorder potential competes with elastic forces, either due to tilt or shear energies. Whereas a detailed understanding of the weak-pinning phenomenology has been developed over the past decade [3], not much progress has been made regarding the strong-pinning situation.

Recent experimental and theoretical interest concentrates on the low-field properties of vortex matter in strongly layered materials such as $\text{Bi}_2\text{Sr}_2\text{Ca}_1\text{Cu}_2\text{O}_8$ (BiSCCO) [4,5,6,7,8], with particular emphasis on the effects of thermal fluctuations, quenched disorder, and their mutual interplay. In this letter, we present a detailed analysis of the phenomenon of strong vortex pinning in layered type-II superconductors and its crossover to the weak-pinning situation due to thermal fluctuations. We assume quenched point-like disorder and concentrate on the decoupled limit where electromagnetic interactions between pancake vortices determine the behavior of vortex matter. We discuss the presence of two step-like features in the current-voltage characteristics (CVC) and determine the evolution in temperature of the two corresponding critical current densities $j_{pc}(T)$ and $j_g(T)$ describing the onset of strong pinning and of glassiness, see Fig. 1. To account for thermal fluctuations smoothing the disorder potential in the strong-pinning regime we introduce the new concept of *variable-range* thermal smoothing. We show how the thermal depinning of vortices proceeds in a sequence of steps until the usual weak collective pinning situation is recovered at high temperatures. Furthermore, we predict that the strong dispersion in the electromagnetic tilt modulus leads to a pronounced jump

in the critical current density j_g with increasing temperature. The main results of our analysis are summarized in the pinning diagram of Fig. 2 which shows the various pinning regimes present in the low-field region below the field $B_\lambda = \Phi_0/\lambda^2$, where λ is the planar London penetration depth and Φ_0 denotes the flux unit. In a forthcoming publication [9] we will map out the entire pinning diagram and generalize our analysis to include finite Josephson coupling.

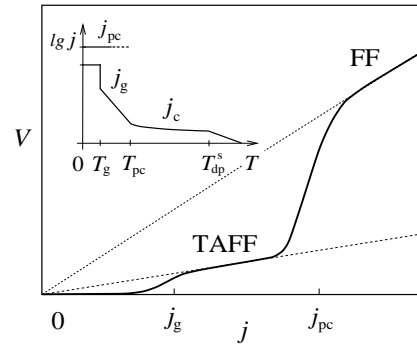


FIG. 1. Current-voltage characteristics of layered superconductors in the pancake-vortex pinning regime ($T < T_{pc}$) exhibiting a two-step behavior. Above the critical current density j_{pc} we find the usual flux-flow (FF) regime with resistivity ρ_{FF} . As the current j drops below j_{pc} , pancake vortices are trapped into potential wells of depth U_{pc} and the system enters a second ohmic regime with a reduced resistivity due to thermally activated flux flow of individual pancake vortices, $\rho_{TAFF} \sim \rho_{FF} \exp(-U_{pc}/T)$. At $j_g < j_{pc}$ the motion of pancake vortices is inhibited by elastic forces, resulting in a sharp drop of the voltage (glassy response). Inset: temperature dependence of the two step features in the CVC. The critical current density j_{pc} remains constant up to $T = U_{pc}$, where the corresponding step in the CVC disappears. The critical current density for glassy response j_g decreases with temperature and, at $T = T_{pc}$, smoothly goes over to the critical current density j_c determined by weak collective pinning theory. Note that $T_{pc} \simeq U_{pc}$ as shown in the text.

We begin our study with the low-field/low-temperature limit and consider an individual vortex line oriented perpendicular to the layers. The presence of point disorder leads to a distortion of the vortex line with a typical relative displacement u between neighboring pancake vor-

tices. The optimal pinning state is determined by the competition between the elastic and the pinning energies. The deformation of the vortex line on a length L costs an energy $\mathcal{E}_{el}(u, L) \simeq \varepsilon_l(u, k_z \simeq 1/L) u^2/L$. For purely electromagnetic interaction (uncoupled layers) the elasticity ε_l takes the strongly dispersive form $\varepsilon_l(u < \lambda, k_z) = (\varepsilon_o/2\lambda^2 k_z^2) \ln[1 + \lambda^2 k_z^2/(1 + u^2 k_z^2)]$, with the line energy $\varepsilon_o = (\Phi_o/4\pi\lambda)^2$. Here, we have interpolated between the formulae valid for $uk_z > 1$ [1] and $uk_z < 1$ [3]. On the other hand, adjusting to the disorder potential, a vortex segment of length L gains the pinning energy $\mathcal{E}_{pin}(u, L) \simeq |\mathcal{E}_0(u)|\sqrt{L/d}$, where d is the layer separation and $\mathcal{E}_0(u)$ is the deepest minimum a pancake vortex can settle in within the area u^2 . This energy is determined by the condition $u^2 \int^{\mathcal{E}_0} g(\mathcal{E}) d\mathcal{E} \simeq 1$, where $g(\mathcal{E})$ is the distribution of pinning energies, which for a large number of defects we assume to be Gaussian [8]

$$g(\mathcal{E}) = \frac{1}{\sqrt{\pi}U_p \xi^2} \exp\left(-\frac{\mathcal{E}^2}{U_p^2}\right). \quad (1)$$

Here, U_p quantifies the disorder strength and ξ is the planar coherence length (and also the typical distance between pinstates). For $u \gg \xi$ (strong pinning) each pancake vortex can explore many minima and one finds

$$\mathcal{E}_0(u) \simeq -U_p \left[\ln\left(\frac{u^2}{\xi^2}\right) \right]^{1/2} < -U_p. \quad (2)$$

Introducing the energy scale $E_{em} = \varepsilon_o d \xi^2 / \lambda^2$, we arrive at the vortex free energy f per unit length,

$$f(u, L) \simeq \frac{E_{em}}{d} \ln\left(1 + \frac{\lambda^2}{L^2 + u^2}\right) \frac{u^2}{\xi^2} + \frac{\mathcal{E}_0(u)}{d} \sqrt{\frac{d}{L}}. \quad (3)$$

Minimizing f with respect to u and L provides us with the optimal pinning state. For strong pinning the minimum is realized by the 0D pancake-vortex configuration ($L = d$) and minimizing Eq. (3) with respect to u , we obtain the optimal search area [8]

$$u_g^2 \simeq \xi^2 \frac{U_p}{E_{em}} \left[\ln\left(\frac{U_p}{E_{em}}\right) \right]^{-1/2} \left[\ln\left(\frac{\lambda^2 E_{em}}{\xi^2 U_p}\right) \right]^{-1}. \quad (4)$$

The activation barrier for pancake-vortex motion is

$$U_{pc} = -\mathcal{E}_0(u_g) \simeq U_p \left[\ln\left(\frac{U_p}{E_{em}}\right) \right]^{1/2}. \quad (5)$$

Comparing the Lorentz force $j(\Phi_o/c)d$ with the pinning force U_{pc}/ξ , we find the pancake critical current density,

$$j_{pc} \simeq j_p \left[\ln\left(\frac{U_p}{E_{em}}\right) \right]^{1/2}. \quad (6)$$

Here, $j_p = j_o(U_p/\varepsilon_o d)$ and $j_o = c\varepsilon_o/\xi\Phi_o$ denotes the depairing current density. In the weak-pinning situation

$U_p < E_{em}$ we have $u_g \simeq \xi$, $\mathcal{E}_0 \simeq -U_p$, and it is energetically more favorable for the system to settle in the 1D pinning regime: Minimizing $f(u = \xi, L)$ with respect to L , we find $L_c \simeq \lambda(\lambda/d)^{1/3}(E_{em}/U_p)^{2/3} > \lambda$. The parameter U_p can be estimated from experiments measuring the critical current density at low B and T and is typically of the order of 10 K (BiSCCO). In comparison, the electromagnetic elastic energy $E_{em} \approx 0.2$ K is much smaller. From these estimates we conclude that we usually encounter a strong-pinning situation with $U_p \gg E_{em}$ in strongly layered high- T_c material.

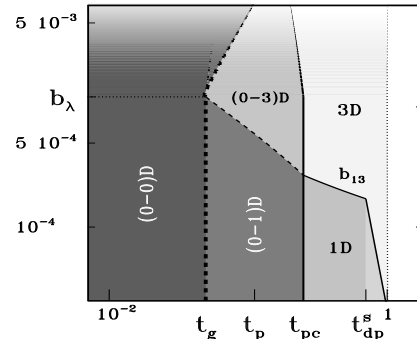


FIG. 2. B - T -pinning diagram of a layered superconductor with decoupled layers (log scales, $t = T/T_c$, $b = B/B_{c2}$; $B_{\lambda} = \Phi_o/\lambda^2$; parameters for BiSCCO: $\lambda = 1800$ Å, $\xi = 25$ Å, $d = 15$ Å, $T_c = 90$ K). Results for the various pinning regimes are shown for moderate pinning with $T_p = U_p = 10$ K. The strong-pinning region at low temperatures $T < T_{pc}$ is divided into two parts: At $T < T_g$ thermal effects are irrelevant [(0-0)D regime], while at $T_g < T < T_{pc}$ variable-range thermal smoothing takes place [(0-1)D and (0-3)D regimes]. The dashed fat line at $T = T_g$ indicates the jump in the collective pinning length L_g and the critical current density j_g . At temperatures $T > T_{pc}$ and low inductions vortex segments of length $L_c > \lambda$ are pinned collectively (1D regime). The remaining area shows the 3D (vortex-bundle) pinning regime.

The strong pinning of individual pancake vortices into potential wells of depth U_{pc} leads to a sharp drop in the current-voltage characteristics (CVC) at the critical current density j_{pc} , see Fig. 1. However, at finite temperatures the CVC does not drop to zero, as the individual pancake vortices can overcome their finite pinning barriers by thermal activation, and we arrive at a second ohmic regime at small current densities $j < j_{pc}$ with a reduced resistivity described by thermally activated flux flow $\rho_{TAFF} \sim \rho_{FF} \exp(-U_{pc}/T)$ [here, $\rho_{FF} = (B/H_{c2})\rho_n$ is the usual flux-flow resistivity, with H_{c2} the upper critical field and ρ_n the normal-state resistivity]. Glassy response appears only at low current densities $j < j_g \ll j_{pc}$, when the free thermal hopping of pancake vortices is inhibited by the elastic coupling to other pancake vortices. To determine j_g we have to consider the hopping process of individual pancake vortices. Following the usual variable-range-hopping (VRH) argument [10], a pancake vortex can move freely as long as the current compensates for

the energy $\delta\mathcal{E}(u)$ required to hop on to the next favorable state. The ‘‘minigap’’ $\delta\mathcal{E}(u)$ is obtained from comparing neighboring favorable states: With $u^2 \int^{\mathcal{E}_1} d\mathcal{E}g(\mathcal{E}) = 2$ we find $\delta\mathcal{E}(u) = \mathcal{E}_1 - \mathcal{E}_0 \simeq U_p [\ln(u^2/\xi^2)]^{-1/2}$. The onset of glassy response is determined by the condition $j_g(\Phi_o/c) u_g d \simeq \delta\mathcal{E}(u_g)$, resulting in the critical current density

$$j_g \simeq j_p \left(\frac{E_{\text{em}}}{U_p} \right)^{1/2} \left[\ln \left(\frac{U_p}{E_{\text{em}}} \right) \right]^{-1/4}, \quad (7)$$

and the corresponding pinning energy

$$U_g = \delta\mathcal{E}(u_g) \simeq U_p \left[\ln \left(\frac{U_p}{E_{\text{em}}} \right) \right]^{-1/2}. \quad (8)$$

As the external current j decreases below j_g , *single* pancake vortices cannot find an appropriate final state any more and vortex motion involves line segments with a length determined by the usual laws of creep dynamics [3], $L(j) \simeq L_g(j_g/j)^{5/7}$ (here, $L_g = d$).

Going over to finite temperature, we note that the situation remains unchanged for $T < U_g$ [(0-0)D regime]. As T increases beyond U_g , the process of variable-range thermal smoothing (VRS) sets in: Thermal fluctuations push the vortices to probe an area $\langle u^2 \rangle_{\text{th}} > u_g^2$, but elastic forces prevent individual pancake vortices from hopping to favorable states, hence segments of length $L_g(T) > d$ will take over the creep process. The thermal hopping of these segments then leads to the smoothing of the pinning energy. Hence, the temperature $T_g = U_g$ defines a (first) thermal depinning temperature in our problem.

We proceed with a detailed analysis of VRS: The mean-squared thermal displacement of a free vortex segment of length L is given by $\langle u^2(L, T) \rangle_{\text{th}} = \int_{1/L}^{1/d} (dk_z/2\pi) (T/\varepsilon_l(k_z)k_z^2)$, and using the dispersive elasticity from above, we find

$$\langle u^2(L, T) \rangle_{\text{th}} \simeq \begin{cases} \xi^2 \frac{T}{E_{\text{em}}}, & d < L < \lambda^2/d, \\ \xi^2 \frac{T}{E_{\text{em}}} \frac{dL}{\lambda^2}, & \lambda^2/d < L, \end{cases} \quad (9)$$

[for $d < L < u$ we should account for a log-correction $\ln[(\lambda/\xi)^2 E_{\text{em}}/T]$ guaranteeing the smooth crossover to u_g^2 as $(L, T) \searrow (d, T_g)$]. The thermally smoothed pinning energy for a vortex segment of length L is given by [9]

$$\mathcal{E}_{\text{pin}}(L, T) \simeq \sqrt{\frac{\langle (\Delta\mathcal{E})^2(T) \rangle}{N(T)}} \sqrt{\frac{L}{d}}, \quad T > T_g. \quad (10)$$

Here, $\langle (\Delta\mathcal{E})^2 \rangle = \langle \mathcal{E}^2 \rangle - \langle \mathcal{E} \rangle^2$ denotes the fluctuation in the pinning energy [use Eq. (1)], which is equal to U_g^2 at $T = T_g$ and tends to $U_p^2/2$ as $T \rightarrow \infty$. $N(T)$ is the number of available states given the search area $\langle u^2 \rangle_{\text{th}}$, $N(T) \approx \langle u^2 \rangle_{\text{th}} \int_{\mathcal{E}_0}^{\mathcal{E}_0+T} d\mathcal{E}g(\mathcal{E})$, with lower and upper limits $N(T_g) = 1$ and $N(T \rightarrow \infty) = \langle u^2 \rangle_{\text{th}}/\xi^2$. It is the

suppression in the number of available states, $N(T) \ll \langle u^2 \rangle_{\text{th}}/\xi^2$, which distinguishes the new VRS from the conventional smoothing occurring within weak collective pinning theory [11]. This reduced smoothing is a consequence of strong pinning and is realized within the regime $T < T_{\text{pc}}$, where the (second) depinning temperature T_{pc} is determined by the condition $N(T_{\text{pc}}) \approx \langle u^2 \rangle_{\text{th}}/2\xi^2$. For the distribution (1) we find $T_{\text{pc}} \simeq U_{\text{pc}}$. At $T > T_{\text{pc}}$ the entire set $N(T) \simeq \langle u^2 \rangle_{\text{th}}/\xi^2$ of pinning states takes part in the smoothing and Eq. (10) reproduces the standard expression [11], $\mathcal{E}_{\text{pin}}(L, T) \simeq U_p \sqrt{\xi^2/\langle u^2 \rangle_{\text{th}}} \sqrt{L/d}$.

Within the VRS regime at low temperatures $T_g < T < T_{\text{pc}}$ we use suitable numerical interpolations for the error function [from $\int_{\mathcal{E}_0}^{\mathcal{E}_0+T} d\mathcal{E}g(\mathcal{E})\mathcal{E}^n$, ($n = 0, 2$)],

$$N(T) \approx \left(\frac{T}{T_g} \right)^{1/2} \exp \left(\frac{T}{T_g} \right), \quad \langle (\Delta\mathcal{E})^2(T) \rangle \approx T_g T, \quad (11)$$

such that $\mathcal{E}_{\text{pin}}(d, T)$ goes over to U_g and $U_p \sqrt{\xi^2/\langle u^2 \rangle_{\text{th}}}$ as $T \searrow T_g$ resp. $T \nearrow T_{\text{pc}}$. The vortex free energy f per unit length takes the form

$$f(L, T) \simeq \frac{E_{\text{em}}}{d} \ln \left(1 + \frac{\lambda^2}{L^2} \right) \frac{\langle u^2 \rangle_{\text{th}}}{\xi^2} - \frac{T}{d} \left(\frac{T_g}{T} \right)^{3/4} \exp \left(-\frac{T}{2T_g} \right) \sqrt{\frac{d}{L}}. \quad (12)$$

Again, the minimum of f with respect to L defines the pinning length L_g . Inspection of Eq. (12) reveals that the minimum at $L = d$ vanishes at $T = T_g$, implying that $L_g(T)$ is determined by the minimum at large lengths,

$$L_g(T) \simeq \lambda \left(\frac{\lambda}{d} \right)^{1/3} \left(\frac{T}{T_g} \right)^{1/2} \exp \left(\frac{T}{3T_g} \right) < \lambda^2/d. \quad (13)$$

The jump from $L_g = d$ to $L_g(T) > \lambda$ at $T = T_g$ implies a concurring jump in the pinning energy and the critical current density,

$$U_g(T) \simeq T \left(\frac{\lambda}{d} \right)^{2/3} \left(\frac{T_g}{T} \right)^{1/2} \exp \left(-\frac{T}{3T_g} \right), \quad (14)$$

$$j_g(T) \simeq j_g \left(\frac{d}{\lambda} \right)^{2/3} \left(\frac{T_g}{T} \right)^{1/2} \exp \left(-\frac{2T}{3T_g} \right). \quad (15)$$

The jump at T_g is a consequence of the strong dispersion in the electromagnetic line tension and persists into the high-field regime [9], where it matches up with the jump found by Kes and Koshelev [12] in their $T = 0$ analysis of this problem. A sharp increase (jump) in the activation energy U by a factor of 10 with increasing temperature ($T \gtrsim 15$ K) has been found in several relaxation experiments in BiSCCO material [13].

At temperatures above T_{pc} we can ignore the underlying strong pinning. Repeating the above minimization procedure with the usual smoothed pinning potential [11], we obtain the weak-pinning results (1D regime)

$$L_c(T) \simeq \lambda \left(\frac{\lambda}{d} \frac{T^3}{E_{\text{em}} U_p^2} \right)^{1/3} = \lambda \frac{\lambda}{d} \frac{T}{T_{\text{dp}}^s}, \quad (16)$$

$$U_c \simeq \left(\frac{\lambda^2}{d^2} E_{\text{em}} U_p^2 \right)^{1/3} = T_{\text{dp}}^s, \quad (17)$$

$$j_c(T) \simeq j_p \left(\frac{d^5 E_{\text{em}}^2}{\lambda^5 U_p^2} \right)^{1/3} \left(\frac{T_{\text{dp}}^s}{T} \right)^{3/2}, \quad (18)$$

where we have introduced the single-vortex depinning temperature T_{dp}^s . Quick inspection shows that $L_c(T)$, U_c , and $j_c(T)$ match up with $L_g(T)$, $U_g(T)$, and the onset of glassy response at $j_g(T)$ when $T \searrow T_{\text{pc}}$.

When the collective pinning length $L_c(T)$ exceeds λ^2/d the mean thermal displacement grows with increasing length and pinning becomes marginal [3]. The determination of $L_c(T)$ involves the calculation of the disorder-induced fluctuations $\langle\langle u_p^2(L, T) \rangle\rangle$, where $\langle\langle \cdot \rangle\rangle$ denotes averaging over thermal fluctuations and disorder. Repeating this calculation for the case of electromagnetic coupling, we find $\langle\langle u_p^2(L, T) \rangle\rangle / \xi^2 \simeq (U_p/T)^2 (L/d) \ln(Ld/\lambda^2)$. As the disorder-induced fluctuations increase beyond the thermal ones, the system crosses over to the pinning-dominated regime. The condition $\langle\langle u_p^2(L, T) \rangle\rangle \simeq \langle u^2(L, T) \rangle_{\text{th}}$ determines the length

$$L_c(T) \simeq \lambda \frac{\lambda}{d} \exp \left(\frac{T}{T_{\text{dp}}^s} \right)^3, \quad (19)$$

and the critical current density takes the form

$$j_c(T) \simeq j_p \left(\frac{d^5 E_{\text{em}}^2}{\lambda^5 U_p^2} \right)^{1/3} \sqrt{\frac{T}{T_{\text{dp}}^s}} \exp \left[-\frac{3}{2} \left(\frac{T}{T_{\text{dp}}^s} \right)^3 \right]. \quad (20)$$

The above results properly match the previous ones at the crossover temperature $T = T_{\text{dp}}^s$. The complete temperature dependencies of the (critical) current densities j_{pc} , j_c , and j_g are illustrated in the inset of Fig. 1.

As we increase the magnetic field, interactions with other vortices start to interfere with the accommodation of the individual vortices to the disorder potential. The regime of validity of the above results is found by comparing the tilt elastic energy $E_{\text{em}}(u/\xi)^2$ with that of shear, $c_{66}u^2d$, with the shear modulus given by $c_{66} \simeq \varepsilon_o/a_o^2$ and $(\varepsilon_o/\lambda^2)\sqrt{\lambda/a_o} \exp(-a_o/\lambda)$ above resp. below B_λ . At low temperatures $T < T_g$ we find that pancake vortices start to interact within the planes as the magnetic induction increases beyond B_λ , see Fig. 2. At $T > T_g$ we have to account for the finite lengths $L_g(T)$ and $L_c(T)$ of the segments involved. The crossover condition $L \simeq \lambda \exp(a_o/2\lambda)$ produces the result

$$B_{13}(T) \simeq B_\lambda \left(\frac{T}{T_g} + \ln \frac{\lambda}{d} \right)^{-2}, \quad T_g < T < T_{\text{pc}}, \quad (21)$$

$$B_{13}(T) \simeq B_\lambda \ln^{-2} \left(\frac{\lambda}{d} \frac{T^3}{E_{\text{em}} U_p^2} \right), \quad T_{\text{pc}} < T < T_{\text{dp}}^s, \quad (22)$$

$$B_{13}(T) \simeq B_\lambda \left(\ln \frac{\lambda^2}{d^2} \right)^{-2} \left(\frac{T_{\text{dp}}^s}{T} \right)^6, \quad T_{\text{dp}}^s < T. \quad (23)$$

Above $B_{13}(T)$ pinning involves relaxation of vortex bundles [(0-3)D and 3D regimes]. These results apply to the vortex solid regime below the melting line $B_m(T)$ [14]: Upon melting, both the shear and tilt moduli vanish in the resulting pancake-vortex gas phase, cutting off the 1D and 3D pinning regimes at $B_m(T)$.

Our analysis (and its generalization to higher fields [9]) sheds light on two recent experiments in layered BiSCCO material. The Maley analysis of the creep barrier as measured by van der Beek *et al.* [4] is consistent with a diverging barrier $U(j \rightarrow 0) \rightarrow \infty$, rather than the constant barrier expected for strong pancake pinning in the low- T /low- B domain. The above results explain how individual pancake vortices couple into vortex lines exhibiting diverging barriers as the driving force vanishes. Second, recent local Hall-probe measurements of the current flow in BiSCCO crystals show a sharp, roughly field-independent onset of bulk pinning as the temperature decreases below $T \approx 40$ K [6]. This experimental finding is in agreement with the appearance of strong non-linearities in the CVC below the temperature T_{pc} , see Fig. 1. The definite identification of this pinning onset with either j_{pc} or j_g requires a detailed amplitude and frequency analysis of the experimental feature.

We thank A.E. Koshelev, M. Nideröst, and A. Suter for stimulating discussions, and the Swiss National Foundation for financial support.

-
- [1] J.R. Clem, Phys. Rev. B **43**, 7837 (1991).
 - [2] A.I. Larkin and Yu.N. Ovchinnikov, J. Low Temp. Phys. **34**, 409 (1979).
 - [3] G. Blatter *et al.*, Rev. Mod. Phys. **66**, 1125 (1994).
 - [4] C.J. van der Beek *et al.*, Physica C **192**, 307 (1992).
 - [5] E. Zeldov *et al.*, Nature (London) **375**, 373 (1995) and Europhysics Lett. **30**, 367 (1995).
 - [6] D.T. Fuchs *et al.*, unpublished.
 - [7] D. Ertas and D.R. Nelson, Physica C **272**, 79 (1996); T. Gi-amarchi and P. Le Doussal, Phys. Rev. B **55**, 6577 (1997).
 - [8] A.E. Koshelev *et al.*, Phys. Rev. B **53**, 2786 (1996); A.E. Koshelev and V.M. Vinokur, preprint cond-mat/ 9801144.
 - [9] G. Burkard, O.S. Wagner, V.B. Geshkenbein, and G. Blatter, unpublished.
 - [10] A.L. Efros and B.I. Shklovskii, *Electronic Properties of Doped Semiconductors*, (Springer, Berlin, 1984).
 - [11] M.V. Feigel'man and V.M. Vinokur, Phys. Rev. B **41**, 8986 (1990).
 - [12] A.E. Koshelev and P. Kes, Phys. Rev. B **48**, 6539 (1993).
 - [13] V.N. Zavaritzky and N.V. Zavaritzky, Physica C **185** – **189**, 2141 (1991); V.V. Metlushko *et al.*, Physica B **194** – **196** 2219 (1994); M. Nideröst *et al.*, Phys. Rev. B **53**, 9286 (1996).
 - [14] G. Blatter *et al.*, Phys. Rev. B **54**, 72 (1996).